$CONF-880546--11$

TITLE   NEW DEVELOPMENTS IN THE GNASH NUCLEAR THEORY CODE

AUTHOR(S)   Edward D. Arthur, ██ T. Do
             Phillip G. Young, T-2
             Constance Kalbach-Walker, T-2 Consultant

DISCLAIMER

Los Alamos
Los Alamos National Laboratory
Los Alamos, New Mexico 87545

NEW DEVELOPMENTS IN THE GNASH NUCLEAR THEORY CODE

Edward D. Arthur, Phillip G. Young

Los Alamos National Laboratory, Los Alamos, New Mexico, USA

C. Kalbach

Duke University, Durham, North Carolina, USA

Abstract: During the past year significant improvements have been made to the GNASH nuclear model code system that will be described in this paper. New features such as use of the Ignatyuk level-density model, inclusion of multistage preequilibrium reaction contributions, and approximations to Hauser-Feshbach models will be described and results illustrated. Of particular importance are models developed that describe gamma-ray emission competition relative to particle emission in full detail even for higher energy reaction processes. In addition to these model improvements, the code has been expanded to include up to 300-400 reaction paths in one calculation with options for simple, automatic problem setups. Also, a preliminary formulation of the Kalbach angular distribution phenomenology has been implemented that provides the capability for reasonably accurate calculations of double-differential cross sections and spectra. Calculational examples using the code options will be provided and comparisons to new higher energy neutron and proton measurements will be made.

(keywords: preequilibrium, statistical models, level densities, angular distribution phenomenology)

Introduction

An extensive effort is underway within the Applied Nuclear Science Group at Los Alamos to develop data libraries appropriate for particle energies up to 100 MeV. A principal tool used for such library development has been the GNASH[1] nuclear model code. In order to allow its effective use at higher energies, both from a physics and computational standpoint, a number of substantial improvements have been made. These developments will be discussed within this paper. Comparisons will also be made with available experimental data to illustrate their validity.

Preequilibrium Model Extensions

Comparison with experimental particle emission spectra for incident energies above 50 MeV has indicated the need to incorporate effects resulting from the diffusivity of the nuclear surface into preequilibrium models. Such additions are necessary to match such data, especially for higher emission energy portions of such spectra. Kalbach[2] has developed a phenomenological method for accounting for such nuclear surface effects which has been implemented into GNASH. Basically the excitation energy available to a hole degree of freedom is limited by the assumption of a shallower depth of the nuclear potential at the nuclear surface. Hole degrees of freedom having excitation energies exceeding the effective well depth are excluded from the normally calculated state densities. Schematically if $\omega(p,h,E,\infty)$ represents the state densities determined without consideration of such restrictions, then it must be multiplied by a surface correction factor $f(p,h,E,V)$ to produce the state density suitable for use in the calculation. This factor is given by

$$f(p,h,V,E) = \sum_{i=0}^{h} (-1)^i \begin{bmatrix} h \\ i \end{bmatrix} \left[\frac{E-iV}{E} \right]^{h-1} \Theta(E-iV) \qquad (1)$$

where E is the excitation energy, V is the nuclear well depth relative to the Fermi level, and p,h refer to particle and hole degrees of freedom. Θ is zero for a negative argument and unity otherwise. To determine the effective well depth as a function of projectile energy, Kalbach has fitted higher emission spectra data to arrive at the following expression for V

which is applied when h =1. Otherwise V = 38 MeV. The effect of inclusion of this surface effect approximation is illustrated in Fig 1. where a comparison is made with 90 MeV ^{58}Ni (p,xn) spectra data[3]. At the higher end of the emission spectra this correction increases the calculated value by more than a factor of two, thereby improving significantly the agreement with the data.

A second area of preequilibrium development centered around implementation of a nonequilibrium emission model in residual nuclei populated initially by preequilibrium reactions. Such multi-reaction stage preequilibrium emission can be calculated within the exciton model through changing the initial population conditions to

$$P_0^* (n^* = n\text{-}b) = W_b(n,\epsilon_b) \, \tau(n,E) \qquad (3)$$

where b is the particle number involved in the initial preequilibrium emission process. In GNASH closed-form expressions are used to calculate this multiple stage emission process. The cross section for such processes is then given by

$$\frac{d\sigma}{d\epsilon_b} = \sigma_{CN} \sum_{n^*=n_0^*} W_{b'}(n_0^*,\epsilon) \, \tau(n^*,E^*) D(n^*) \qquad (4)$$

where in GNASH the initial exciton numbers extend from 2 to 6 and the sums in the residual systems extend to n_0 +6. The mean lifetime and depletion factors appearing[0] (τ and D respectively) have forms similar to that found in one stage applications of the exciton model except that $E^*=E\text{-}B\text{-}\epsilon_b$. Multistage preequilibrium components are calculated for $\Delta Z = 0,1$ and $\Delta N= 0,1$ from the Z and N of the target system. Inclusion of such multistage effects does not significantly affect the shape of calculated emission spectra below incident energies of 100 MeV, but at energies above 50 MeV yields of specific residual nuclei can be changed significantly.

A final area of improvement associated with nonequilibrium reaction model components has involved their use in the calculation of angle-dependent spectra. Although a generalization of the exciton model to allow angular distribution calculations has been made by implementation of the nucleon-nucleon free scattering kernel (see Ref.4 for details), the principal method used in GNASH for such calculations employs new systematics recently developed by

particle emission spectra data for nucleon, deuteron, helion, and alpha-particle induced reaction data covering the incident energy range from a few MeV to 600 MeV, systematic behaviors of angular distributions were determined. These were expressed in terms of hyperbolic sines and cosines. Specifically the following parameterization was developed for double-differential cross sections

$$\frac{d^2\sigma}{d\varepsilon_b d\Omega} = \frac{1}{4\pi} \frac{d\sigma}{d\varepsilon_b} \frac{a}{\sinh(a)} [\cosh(a\cos\theta) + f_{MSD}\sinh(a\cos\theta)]$$

(5)

Here a is the slope parameter for an angular distribution and f_{MSD} is the fraction of multi-step direct processes. In the GNASH calculations this has been approximated through use of the preequilibrum contribution calculated for the first compound system. A rather simple parameterization was determined for the slope parameter which depends primarily upon the particle emission energy. Such a preliminary form is given by

$$a = 0.04\varepsilon + 1.8 \times 10^{-6} \varepsilon$$ (6)

where ε is related to the particle emission energy. Figure 2 illustrates the systematic behavior of this slope parameter where slopes determined from (p,p'),(p,d), and (α,α') data on ^{56}Fe and ^{58}Ni at differing incident energies are shown as a function of exit energy. Final expressions developed in Ref 5 still retain much of the simplicity of expression (6) although more additional terms have been added to better extend this phenomenology over a wider incident energy range.

Equilibrium Model Development

Because Hauser-Feshbach statistical model calculations become prohibitively expensive at higher incident energies where many possible compound systems are excited to high excitation energies, alternative methods were implemented to deal with equilibrium emission processes. The first was a straightforward application of the Weisskopf-Ewing evaporation theory taking account fully of gamma-ray competition with particle emission using expressions described by Buttner.[6] All other features (use of optical model transmission coefficients, level densities, and discrete level data) associated with the standard GNASH Hauser-Feshbach version were retained. However the code was modified to handle production and deexcitation of 60 compound systems (versus 10 for the standard version) with 6 emissions (n,p,d,t,^{4}He,γ) allowed from each so that up to 360 reaction paths can be included in one calculation. To simplify problem setup and execution, only a range in Z and N away from the target system has to be specified.

Although implementation of a full gamma-ray competition model in the framework of this evaporation model did produce reasonable results when compared with standard GNASH calculations at higher (~50 MeV) energies, deficiencies did occur at lower energies. To correct these, we have also implemented an approximation to Hauser-Feshbach theory known as the "s-wave" approximation.[7] In this model the standard Hauser-Feshbach cross section expression

$$\frac{d\sigma}{d\varepsilon_b} = \frac{\pi}{k^2} \sum_{I=0}^{\infty} (2I+1)T_I(2s_b+1) \sum_{\ell=0}^{\infty} T_b^\ell(\varepsilon) \sum_{j=|I-\ell|}^{I+\ell} \frac{\rho(E,J)}{D}$$

is replaced by

$$\frac{d\sigma}{d\varepsilon_b} = \frac{\pi}{k^2} \sum_{I=0}^{\infty} (2I+1)T_I(2s_b+1) \sum_{\ell=0}^{\infty} (2\ell+1) T_b^\ell \frac{\rho(E,I)}{D}$$

(7)

Here T_I is the transmission coefficient for the Ith partial wave of the projectile, $\rho(E,J)$ is the spin-dependent level density for the residual nucleus, and D is the total width obtained by integrating over all emission energies and all exit channels. The assumption of this approximation that spin distributions in the compound and residual systems are equivalent means that $\rho(E,J)$ can be replaced by $\rho(E,i)$. The spin distribution in the initial compound system is determined by the standard sum over incident channel transmission coefficients available from an optical model calculation. This spin distribution is then projected unchanged throughout the problem. Figure 3 compares the total gamma-ray production cross section calculated for n+^{56}Fe reactions over the energy range up to 50 MeV. Over most of this energy range the pure evaporation model calculation lies significantly below results obtained from a full Hauser-Feshbach calculation. The s-wave approximation calculation agrees well with the full Hauser-Feshbach results even at lower energies. This behavior is confirmed by the comparison of Fig. 4 where the calculated gamma ray production spectra produced by 36-MeV neutrons is shown. Here the s-wave approximation and Hauser-Feshbach results are very similar, while the evaporation model produces a much lower cross section. Additional calculations to those shown in Fig. 3 indicate that the discrepancy associated with the evaporation model lessens significantly at energies greater than 50-60 MeV. Thus for neutron data library calculations, we have generally employed the full Hauser-Feshbach GNASH version for energies below 30 MeV, the s-wave approximation for energies between 30 and 65-70 MeV, and the evaporation model at energies greater than 60-70 MeV.

A final area of model development centered around implementation of the Ignatyuk[8] level density model. This level density model differs from the Gilbert-Cameron[9] and back-shifted Fermi gas[10] models currently implemented in GNASH in that it contains an energy-dependent Fermi gas parameter. Thus a(U) is given by

$$a(U) = a[1 + f(U)\delta W/U]$$ (8)

Introduction of energy dependence in the Fermi gas level density parameter addresses difficulties encountered in level density calculations that result from the propagation of shell effects (occurring at low excitation energies) to high excitation energies. In expression 8, a is the asymptotic value for the Fermi gas parameter which occurs at high energies and δW accounts for shell effects. It is determined via $\delta W = M_{exp}(Z,A)$ - $M_{ld}(Z,A,\alpha)$, where M_{exp} was calculated using the 1977 Wapstra mass compilation[11] and the liquid drop term M_{ld} was evaluated using standard expressions evaluated at a deformation α. The energy dependence of a(U) occurs via the term f(U) which is given by

$$f(U) = 1 - \exp(-\gamma U) ; \gamma = 0.05 \text{ MeV}$$ (9)

This model permits shell effects to be included at low excitation energies while at high energies such effects disappear as a(U) reaches the symptotic value a. This form is in better agreement with results from microscopic Fermi gas models than the assumption of energy independence for a. As an illustration of these effects and the difference obtained via use of the Ignatyuk model versus that of Gilbert-Cameron, Fig. 5 compares level densities calculated for ^{208}Pb using these models. At low excitation energies the models produce similar results, while at high excitation energies there are massive differences. This occurs since ^{208}Pb represents the rather special case of a doubly magic nucleus where the Gilbert-Cameron a value obtained from resonance spacing data is about 8/MeV. On the other hand the asymptotic value of a appearing in the Ignatyuk model is about 30/MeV. Thus the

'range of the Fermi gas parameter occurring in the determination of the Ignatyuk level density extends from 8 to 30/MeV while the Gilbert-Cameron model value remains fixed at 8/MeV. Since the a parameter appears in the exponential of the standard Fermi gas expression, the tremendous difference appearing in Fig. 5 is not totally unexpected. For most nuclei lying away from shell closures the differences are significantly smaller.

Summary Remarks

Calculations in support of higher energy nuclear data library production have necessitated the implementation of several nuclear model and computational improvements to the GNASH code. These allow reasonably fast and accurate calculations of nucleon-induced reaction data over the energy range from a few MeV up to 200-250 MeV. A second paper[12] prepared for presentation at this Conference provides more details concerning the resulting code system as well as additional comparisons with a variety of available experimental data.

Fig. 3. A comparison of total gamma-ray production cross sections for n + ^{56}Fe reactions calculated using Hauser-Feshbach, evaporation, and s-wave approximation models.

Fig. 1. Exciton model for the ^{58}Ni(p,xn) reactions with 90-MeV protons.
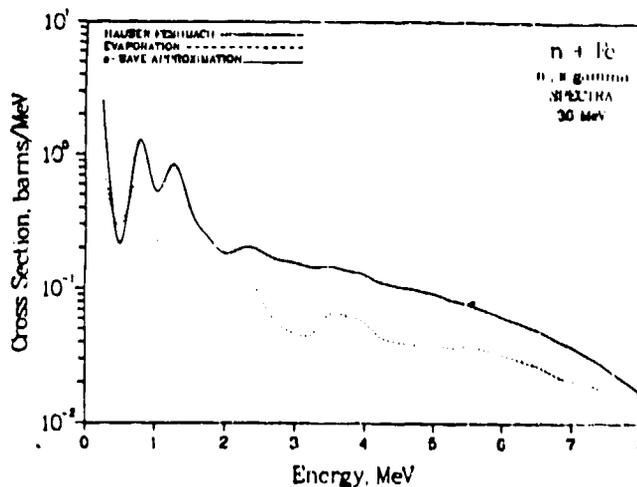
Fig. 4. The gamma-ray production spectra calculated using the three equilibrium models discussed are compared for 36-MeV n + ^{56}Fe reactions.

Fig. 2. The systematic behavior of the slope parameter for continuum angular distributions as determined from charged-particle reaction data
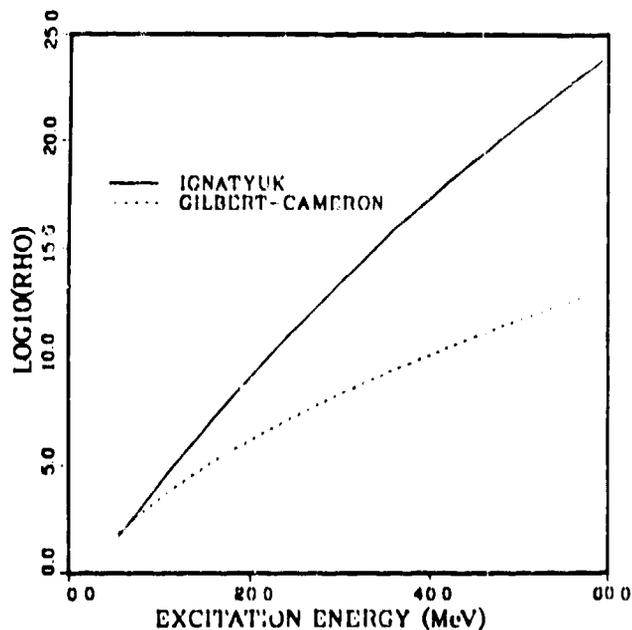
References

1. P. G. Young and E. D. Arthur, LA-6947(1977) and E. D. Arthur, Los Alamos Nat. Lab informal document LA-UR-88-382(1988).

2. C. Kalbach, Phys Rev C $\underline{32}$, 1157(1985).

3. A. M. Kalend et al., Phys Rev C $\underline{28}$, 105 (1983).

4. M. Bozoian, Los Alamos Nat. Lab. informal document LAUR-88-377 (1988)

5. C. Kalbach, LA-UR-87-4139(1987), to be published.

6. H. Buttner et al., Nucl Phys $\underline{63}$, 615(1965).

7. M. Blann and M. Beckerman, Nucleonika $\underline{23}$, 1(1978).

8. A. V. Ignatyuk et al., Sov. J. Nucl. Phys. $\underline{21}$, 255(1976).

9. A. Gilbert and A. G. W. Cameron, Can. J. Phys. $\underline{43}$, 1446 (1965).

10. W. Dilg et al., Nucl. Phys. A $\underline{217}$, 269 (1973).

11. A. H. Wapstra and K. Bos, At. Data and Nuclear Data Tables $\underline{19}$, 175 (1977).

12. E. D. Arthur et al. " Higher Energy Neutron Transport Libraries," contribution to this conference, #A331-R268-A (1988).